Direct and inverse scattering transform analysis of stochastic nonlinear wavefields

Andrey Gelash

1) CNRS-Université Bourgogne Franche-Comté, Dijon, France
2) Skolkovo Institute of Science and Technology, Moscow, Russia.
3) Institute of Automation and Electrometry SB RAS, Novosibirsk, Russia

EGU 2022

DST/IST for analysis and synthesis of nonlinear wave fields

742 Nonlinear Ocean Waves & Inverse Scattering Transform

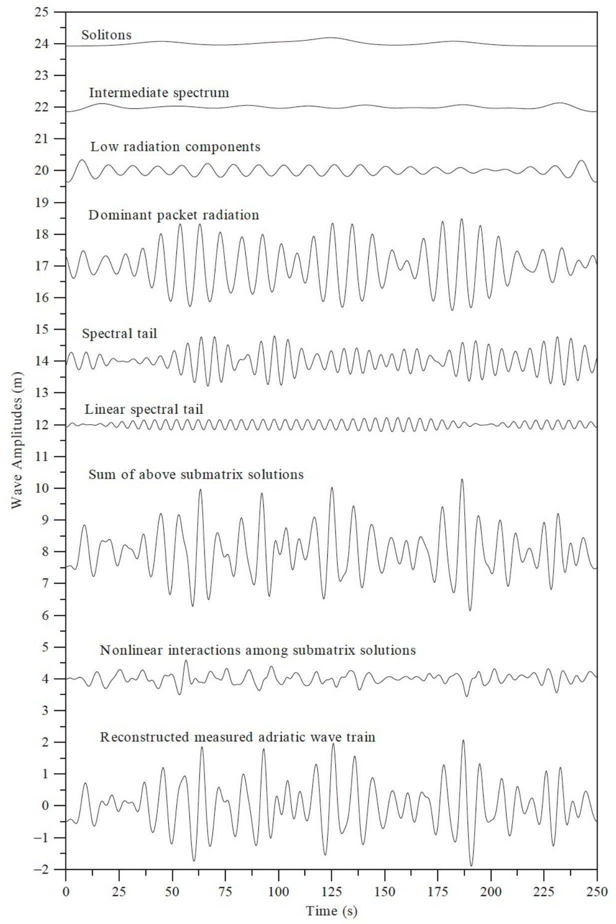

Figure 28.12 Synthesis of the measured Adriatic Sea wave train based upon the submatrix solutions associated with the physical regions of the cnoidal wave spectrum of Figure 28.4.

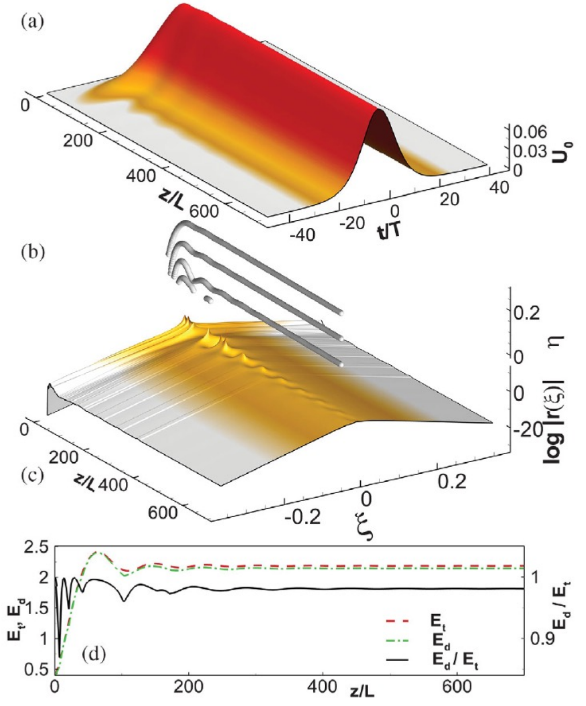

FIG. 4. (a) Evolution of the intensity of the initial pulse having form of the NLSE soliton. Here, $\alpha = 3.5$, $\delta = 0.35$, $\sigma < 0$. (b) Dynamics of the discrete eigenvalues $\{\zeta_n\}$ of nonlinear spectrum for the considered case and (c) the logarithm of the continuous nonlinear spectrum $r(\xi)$ module. (d) Evolution of the total energy E_t, the discrete spectrum energy E_d, and the ratio E_d/E_t.

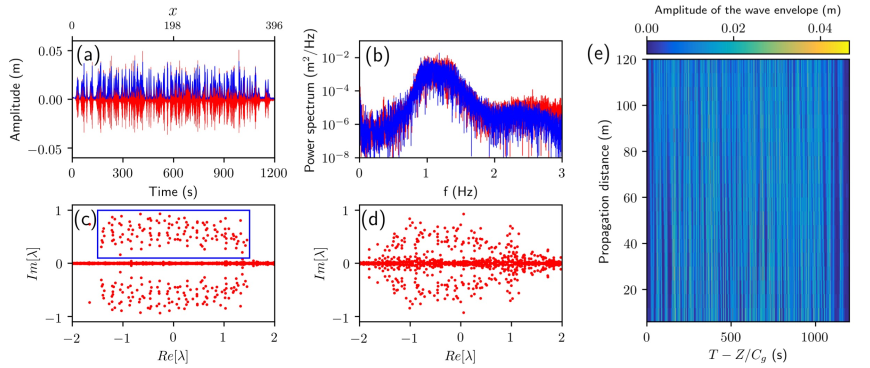

FIG. 2. Gas of $N = 128$ solitons propagating in the 1D water tank. (a) Water elevation (red line) and modulus of the wave envelope measured at $Z_1 = 6$ m, close to the wavemaker. (b) Fourier power spectra of wave elevation at $Z_1 = 6$ m (blue line) and at $Z_{20} = 120$ m (red line). (c) Discrete IST spectrum measured at $Z_1 = 6$ m. (d) Discrete IST spectrum measured at $Z_{20} = 120$ m. (e) Space-time evolution of modulus of the wave envelope recorded by the 20 gauges regularly spaced along the tank. Physical parameters characterizing the experiment are $f_0 = 1.15$ Hz, $k_0 = 5.32$ m^{-1}, $\alpha = 0.936$, $L_{NL} = 45$ m ($\langle|A_0(T)|^2\rangle = 1.58 \times 10^{-4}$ m^2).

P. Suret, et al. Physical Review Letters, (2020).

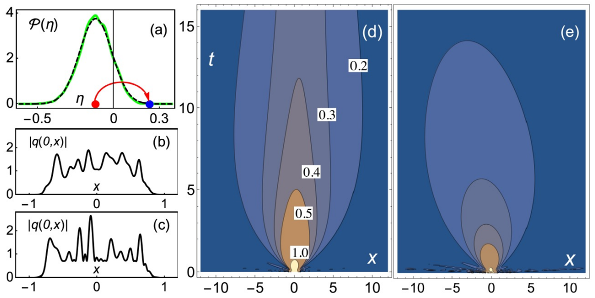

Figure 3: (a) The shift of the nonphysical root to the upper ζ-plane for a particular realization of a real-valued noise within a numerical (green solid) and theoretical (grey dashed) amplitude PDF. Contour plots of $|q(t,x)|$ from numerical simulations of NLSE. Evolution of $q_{\sqcap}$ perturbed by real (b, d) and imaginary (c, e) noise when a soliton is induced and not, respectively. The theoretically predicted and numerically obtained parameters of the induced soliton are $\zeta_{\text{pr}} = 0.223i$, $\zeta_{\text{num}} = 0.232i$ with $\rho_{\text{pr}} = -1.275i$, $\zeta_{\text{act}} = -1.311i$.

A. Osborne, Nonlinear ocean waves, Academic Press, (2010).

I. Chekhovskoy, O. Shtyrina, M. Fedoruk, S. Medvedev, and S. Turitsyn, Physical Review Letters 122, (2019).

R. Mullyadzhanov and A. Gelash, Physical Review Letters, (2021).

Soliton solution of the NLSE

$$\boxed{\psi_{1SS}(x,t) = 2\eta \frac{\exp[-2i\xi(x-x_0) - 2i(\xi^2-\eta^2)t + i\theta']}{ch[2\eta(x-x') + 4\xi\eta t]}}$$

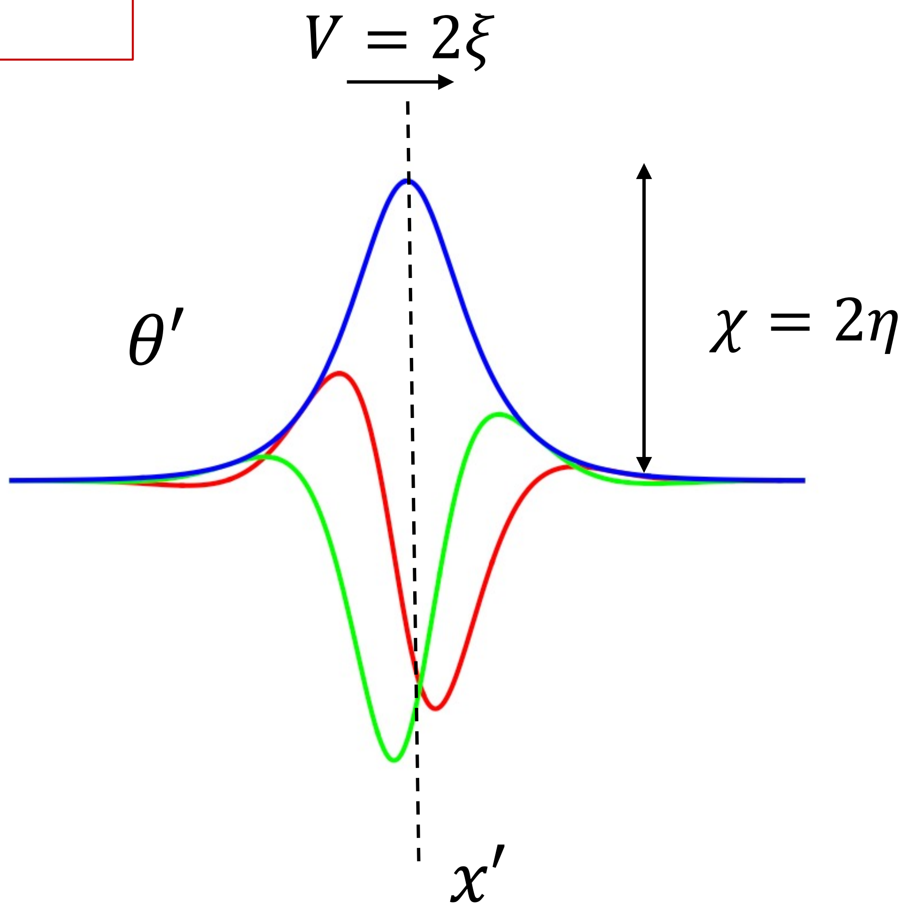

jth soliton complex discrete eigenvalue:

$$\zeta_j = \xi_j + i\eta_j$$

Scattering problem for an arbitrary shaped wave filed

Wave field at a fixed moment of time

$\psi(x, t_0)$

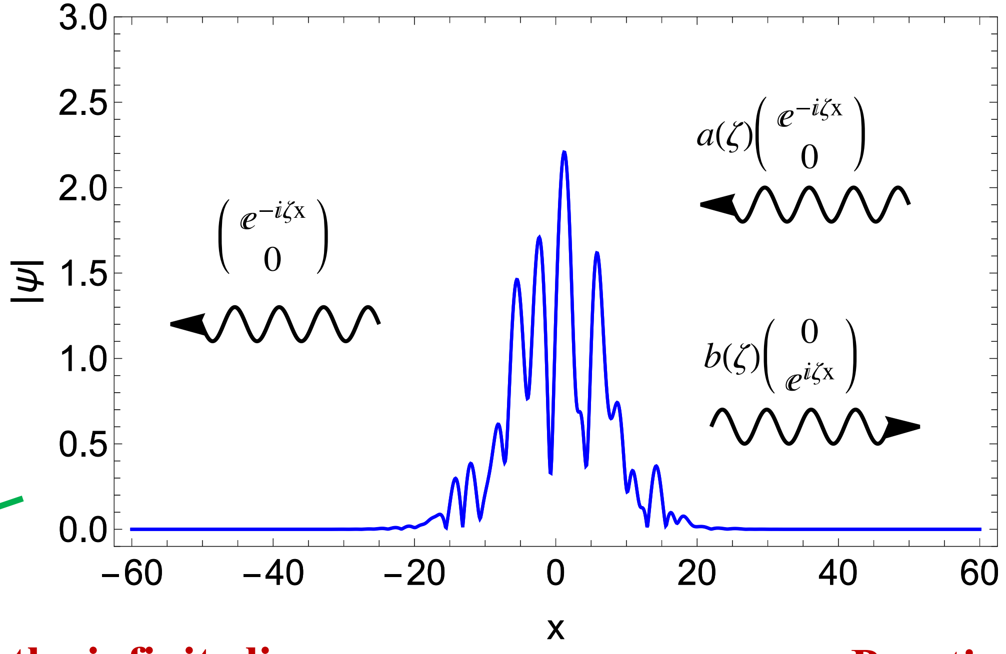

complex-valued spectral parameter of the scattering problem

$\zeta = \xi + i\eta$

Mathematical formulation on the infinite line:

$$\Phi_x = \begin{pmatrix} -i\zeta & \psi \\ -\psi^* & i\zeta \end{pmatrix} \Phi \qquad \text{Zakharov-Shabat system}$$

$$\lim_{x \to -\infty} \Phi = \begin{pmatrix} e^{-i\zeta x} \\ 0 \end{pmatrix}, \quad \lim_{x \to +\infty} \Phi = \begin{pmatrix} a(\zeta) e^{-i\zeta x} \\ b(\zeta) e^{+i\zeta x} \end{pmatrix} \qquad \text{Wave function asymptotics}$$

$$\boxed{\{\, a(\zeta_n) = 0; \qquad \rho_n = \left.\frac{b(\zeta)}{a'(\zeta)}\right|_{\zeta=\zeta_n}; \qquad r(\xi) = \frac{b(\xi)}{a(\xi)} \,\}}$$

Scattering data !

Practical formulation on the interval 2L:

$$\Phi_{tr}(-L) = \begin{pmatrix} e^{-i\zeta L} \\ 0 \end{pmatrix}; \quad \Phi_{tr}(L) = \begin{pmatrix} a_{tr}(\zeta) e^{-i\zeta L} \\ b_{tr}(\zeta) e^{+i\zeta L} \end{pmatrix}$$

$$\begin{pmatrix} \Phi_{tr}(L,\zeta) \\ \Phi'_{tr}(L,\zeta) \end{pmatrix} = S \begin{pmatrix} \Phi_{tr}(-L,\zeta) \\ \Phi'_{tr}(-L,\zeta) \end{pmatrix}$$

$$b_{tr}(\zeta) = S_{21}; \qquad a_{tr}(\zeta) = S_{11} e^{2i\zeta L};$$

$$a'_{tr}(\zeta) = [S_{31} + iL(S_{11} + S_{33})] e^{2i\zeta L}$$

$$\boxed{\{\, a_{tr}(\zeta_n) = 0; \; \rho_n = \left.\frac{b_{tr}(\zeta)}{a_{tr}'(\zeta)}\right|_{\zeta=\zeta_n}; r(\xi) = \frac{b_{tr}(\xi)}{a_{tr}(\xi)} \,\}}$$

Various IST/DST numerical approaches:

- G. Boetta and A. R. Osborne, Journal of Computational Physics 102, 252 (1992).
- S. Burtsev, R. Camassa, and I. Timofeyev, Journal of Computational Physics 147, 166 (1998).
- M. I. Youse and F. R. Kschischang, IEEE Transactions on Information Theory 60, 4312 (2014).
- L. L. Frumin, O. V. Belai, E. V. Podivilov, and D. A. Shapiro, JOSA B 32,290 (2015).
- S. K. Turitsyn, J. E. Prilepsky, S. T. Le, S. Wahls, L. L. Frumin, M. Kamalian, and S. A. Derevyanko, Optica 4, 307 (2017).
- V. Vaibhav, Communications in Nonlinear Science and Numerical Simulation 61, 22 (2018).
- A. Vasylchenkova, J. E. Prilepsky, and S. K. Turitsyn, Optics Letters 43, 3690 (2018).
- V. Aref, S.T. Le & H. Buelow, Journal of Lightwave Technology, 36(6), 1289-1295, (2018).
- F. J. Garca-Gmez and V. Aref, Journal of Lightwave Technology 37, 3563 (2019).
- P. J. Prins and S. Wahls, IEEE Access 7, 122914 (2019).
- S. Medvedev, I. Vaseva, I. Chekhovskoy, and M. Fedoruk, Optics Letters 44, 2264 (2019).
- R. Mullyadzhanov, and A. Gelash, Optics Letters, 44(21), 5298-5301, (2019).
- B. Leible, D. Plabst, N. Hanik, Entropy, 22(10), 1131, (2020).

On behaviour of scattering coefficients a(ζ), $b(\zeta)$ in the ζ- plane

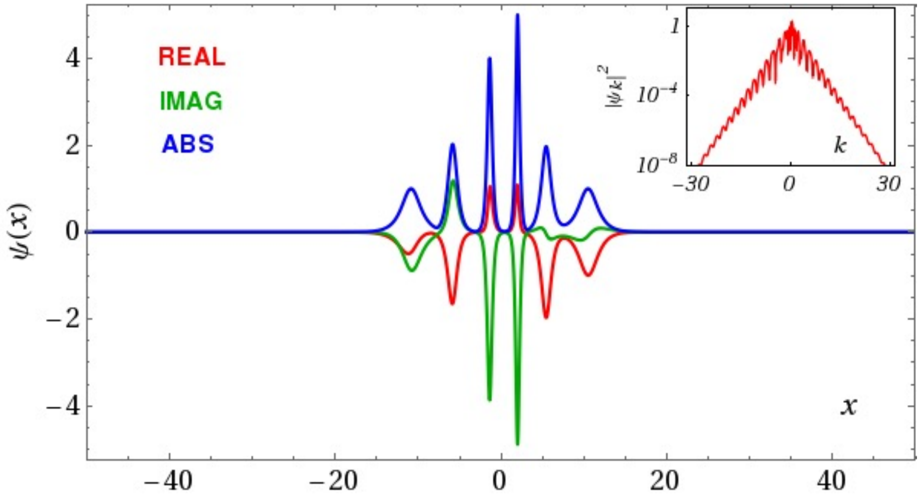

6-soliton solution example

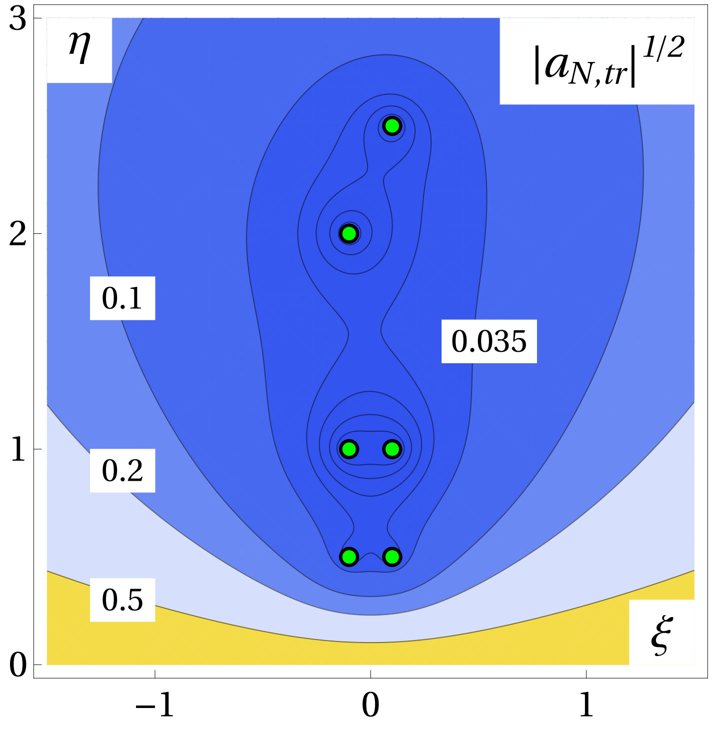

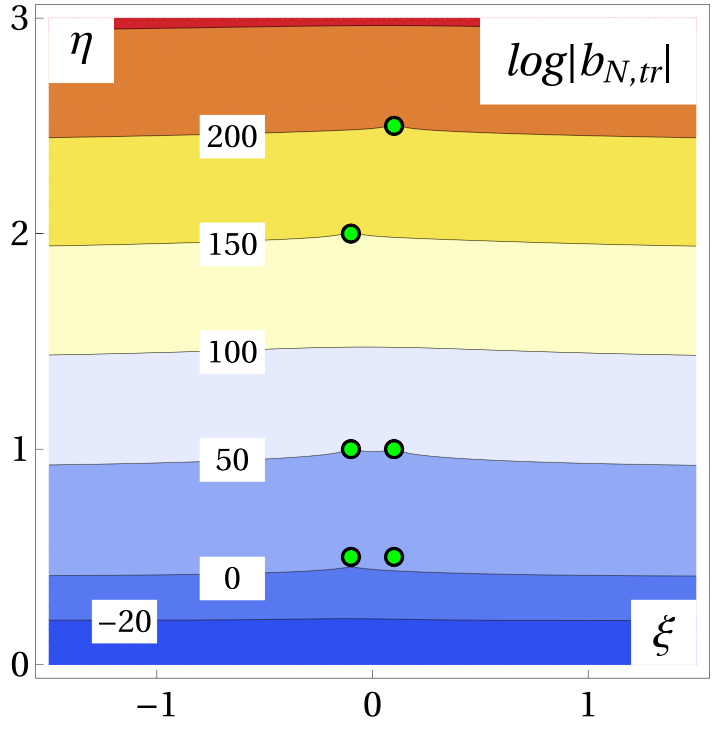

Exact result for the infinite line:

$$a_N(\zeta) = \prod_{k=1}^{N} \frac{\zeta - \zeta_k}{\zeta - \zeta_k^*},$$

$$b(\zeta_n) = \rho_n a_N{}'(\zeta)\Big|_{\zeta=\zeta_n}$$

Leading order answer for the finite interval L:

$$a_{N,tr}(\zeta) = a_N(\zeta) + o_N, \qquad o_N = \mathrm{p}(\zeta)\mathrm{o}(e^{-2\eta_{min}L})$$

$$\boxed{b_{N,tr}(\zeta) = a_N(\zeta) \sum_{k=1}^{N} \frac{\rho_k\, e^{-2i(\zeta-\zeta_k)L}}{\zeta-\zeta_k} + o_N}$$

$$\lim_{L\to\infty} b_{N,tr}(\zeta_k) = b(\zeta_k)$$

Anomalous numerical errors of the direct scattering transform (DST) procedure

Expansion near ζ_k:

$$b_{N,tr}(\zeta_k+\delta\zeta_k)\approx \underbrace{\frac{\rho_k}{\zeta_k-\zeta_k^*}\prod_{j\neq k}^{N}\frac{\zeta_k-\zeta_j}{\zeta_k-\zeta_j^*}}_{\text{I term}}+$$

$$\underbrace{\delta\zeta_k\left(\sum_{l\neq k}^{N}\frac{\rho_l e^{-2i(\zeta_k-\zeta_l)L}}{(\zeta_k-\zeta_l)(\zeta_k-\zeta_k^*)}\prod_{j\neq k}^{N}\frac{\zeta_k-\zeta_j}{\zeta_k-\zeta_j^*}\right)}_{\text{II term}}$$

Dependence of the errors on L:

$$\boxed{\mathrm{error}[\rho_k](L)\sim \text{term II}\sim e^{2(\eta_k-\eta_{min})L}}$$

Critical errors:

$$\boxed{\text{term I}\sim\text{term II}}$$

2-soliton example:

$$\delta\zeta_1^{cr}\sim\frac{\rho_1}{\rho_2}(\zeta_1-\zeta_2)e^{-2i(\xi_2-\xi_1)L}e^{2(\eta_2-\eta_1)L}$$

$$\delta\zeta_2^{cr}\sim\frac{\rho_2}{\rho_1}(\zeta_2-\zeta_1)e^{-2i(\xi_1-\xi_2)L}e^{2(\eta_1-\eta_2)L}$$

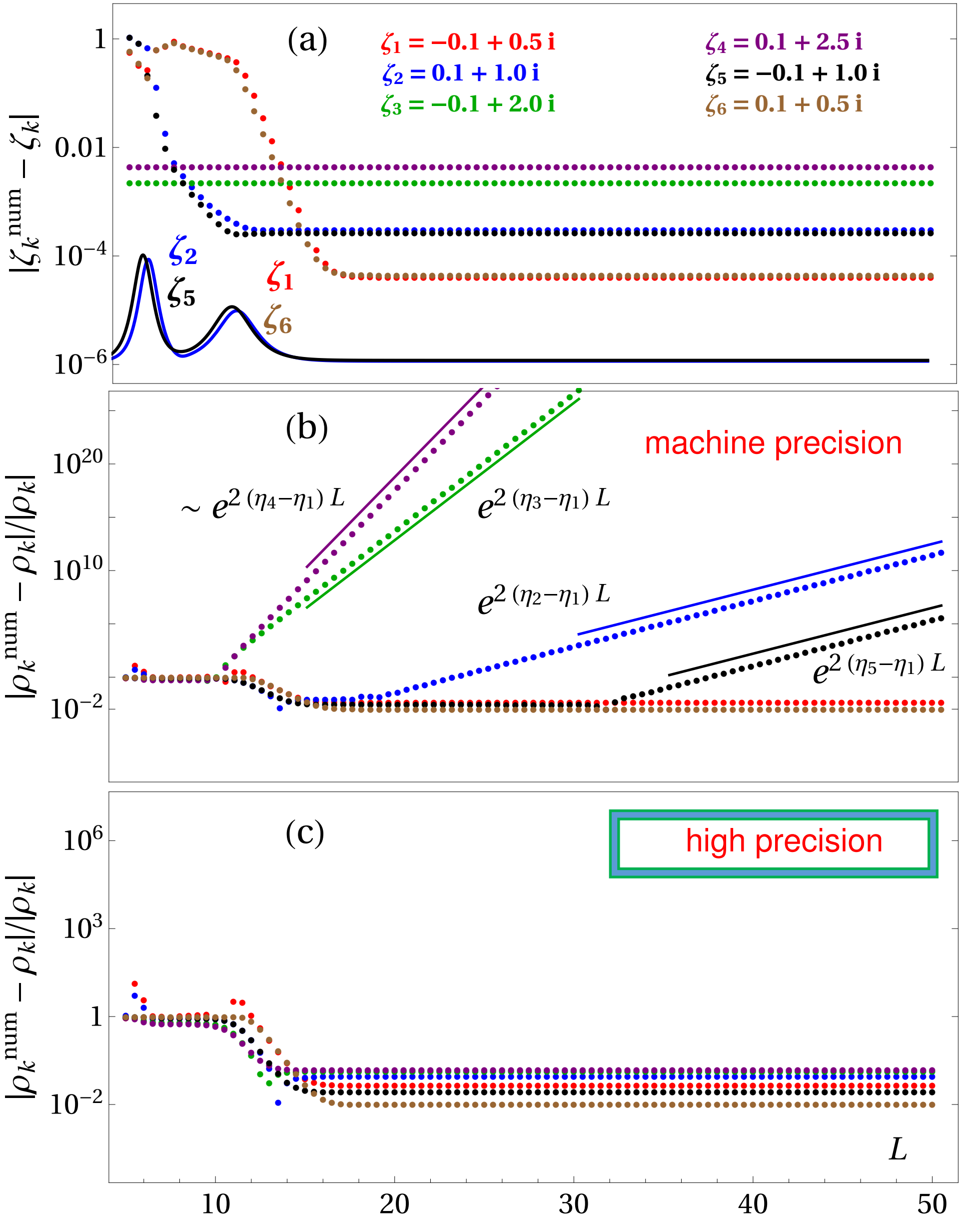

A. Gelash and R. Mullyadzhanov, Anomalous errors of direct scattering transform Physical Review E 101, 052206 (2020).

DST is stable with respect to input wave field distortions, i.e. represents a "well-posed" problem! The anomalous errors can be always fixed using high precision arithmetic.

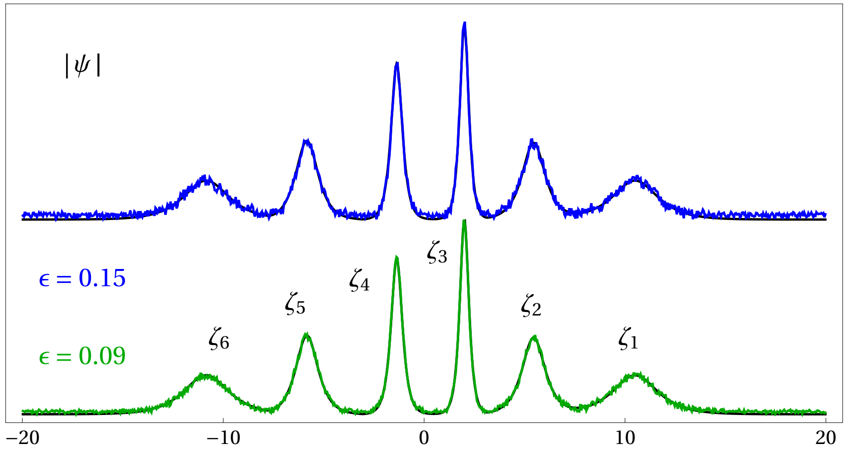

6-soliton solution + noise

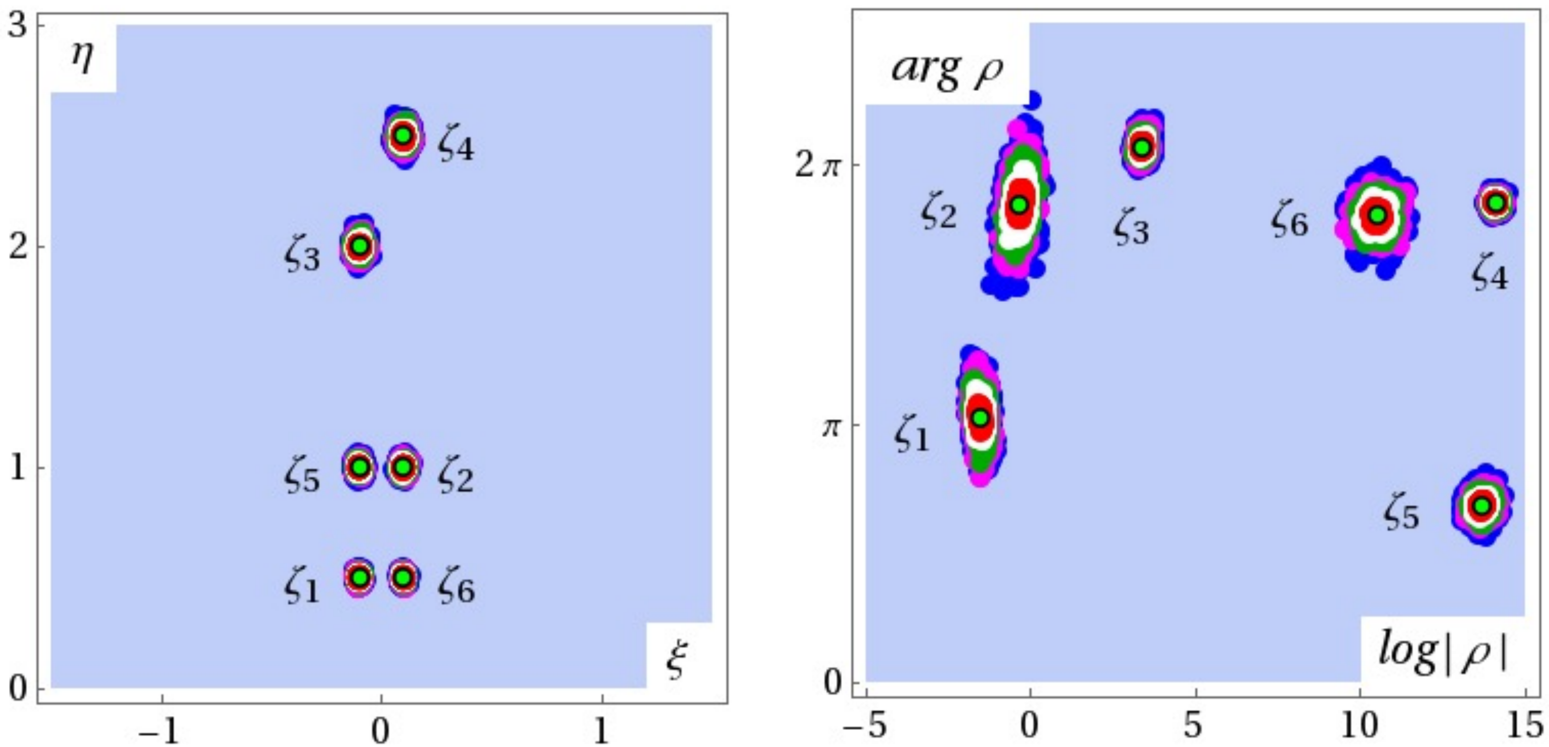

Scattering data recovery for 2000 random noise realizations

Inverse scattering transform for multi-soliton wave field

$$\psi_{NSS}(x,t) = \frac{\det\begin{bmatrix} 0 & q_{1,2} & \cdots & q_{n,2} \\ q_{1,1}^* & \dfrac{(\boldsymbol{q_1}\cdot\boldsymbol{q_1^*})}{\zeta_1+\zeta_1^*} & \cdots & \dfrac{(\boldsymbol{q_1}\cdot\boldsymbol{q_n^*})}{\zeta_1+\zeta_n^*} \\ \vdots & \vdots & \ddots & \vdots \\ q_{n,1}^* & \dfrac{(\boldsymbol{q_n}\cdot\boldsymbol{q_1^*})}{\zeta_n+\zeta_1^*} & \cdots & \dfrac{(\boldsymbol{q_n}\cdot\boldsymbol{q_n^*})}{\zeta_n+\zeta_n^*} \end{bmatrix}}{\det\begin{bmatrix} \dfrac{(\boldsymbol{q_1}\cdot\boldsymbol{q_1^*})}{\zeta_1+\zeta_1^*} & \cdots & \dfrac{(\boldsymbol{q_1}\cdot\boldsymbol{q_n^*})}{\zeta_1+\zeta_n^*} \\ \vdots & \ddots & \vdots \\ \dfrac{(\boldsymbol{q_n}\cdot\boldsymbol{q_1^*})}{\zeta_n+\zeta_1^*} & \cdots & \dfrac{(\boldsymbol{q_n}\cdot\boldsymbol{q_n^*})}{\zeta_n+\zeta_n^*} \end{bmatrix}}$$

$$\boldsymbol{q_j} = (\boldsymbol{e}^{-\phi_j}, \boldsymbol{e}^{+\phi_j})^{\boldsymbol{T}}$$

$$\phi_j = -i\zeta_j\left(x - x_j'\right) - i{\zeta_j}^2 t - i\theta_j'/2$$

We need high precision arithmetic !

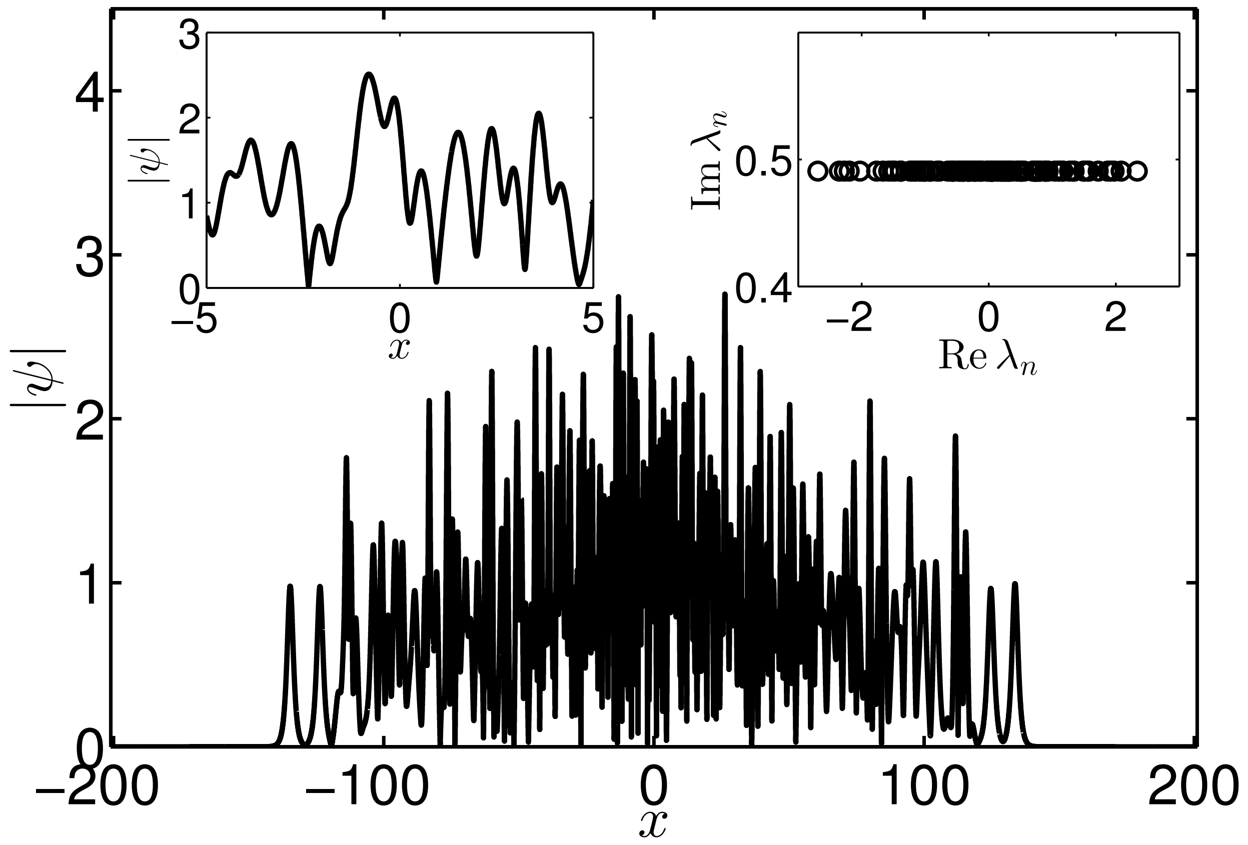

A.A. Gelash, and D.S. Agafontsev, "Strongly interacting soliton gas and formation of rogue waves", Phys. Rev. E, 98, 042210 (2018)

Bound-state soliton gas as the limit of adiabatically growing integrable turbulence

D.S. Agafontsev, A.A. Gelash, R.I. Mullyadzhanov and V.E. Zakharov

In this study, we grow turbulence from small initial noise within the 1D-NLSE equation with linear pumping term,

$$i\psi_t + \psi_{xx} + |\psi|^2 \psi = i p_0 \psi,$$

until different levels of average intensity, and then turn off the pumping and study the resulting integrable turbulence.

Solitonic model of the grown-up wavefields

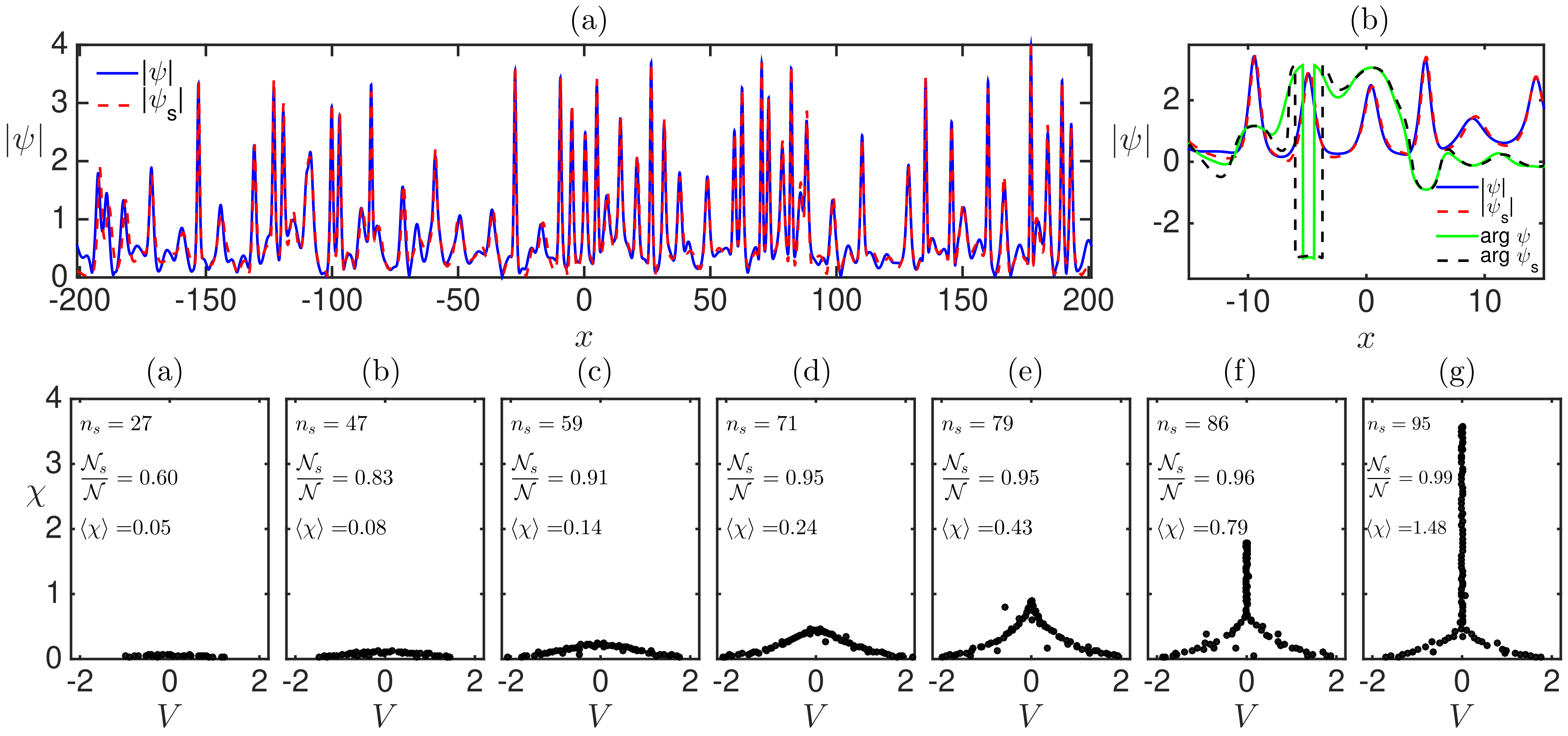

Top row: Grown-up wavefields (blue lines) the corresponding solitonic model (red lines).
Bottom row: Distributions of soliton amplitudes and velocities at different stages of the pumping.

Numerically computed probability distributions of soliton phases and position parameters

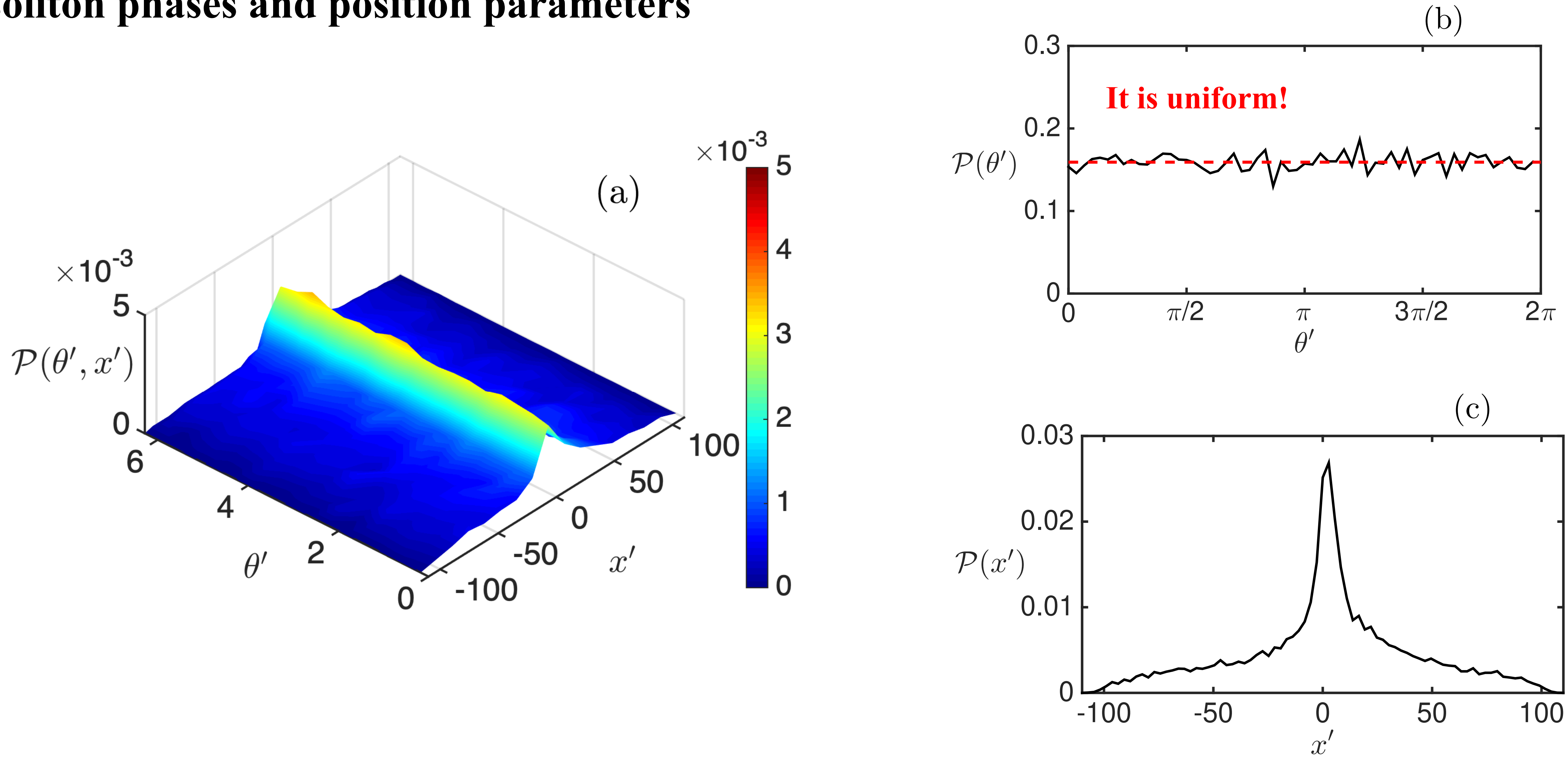

Thank you for your attention!

email: agelash@gmail.com